

Communication: Structure of magnetic lanthanide clusters from far-IR spectroscopy: Tb_n^+ ($n = 5-9$)

John Bowlan,^{1,a)} Dan J. Harding,¹ Jeroen Jalink,² Andrei Kirilyuk,² Gerard Meijer,^{1,2} and André Fielicke¹

¹*Fritz-Haber-Institut der Max-Planck-Gesellschaft, Faradayweg 4-6, 14195 Berlin, Germany*

²*Radboud University Nijmegen, Institute for Molecules and Materials, Heyendaalseweg 135, 6525 AJ Nijmegen, The Netherlands*

(Received 27 November 2012; accepted 4 January 2013; published online 15 January 2013)

Small lanthanide clusters have interesting magnetic properties, but their structures are unknown. We have identified the structures of small terbium cluster cations Tb_n^+ ($n = 5-9$) in the gas phase by analysis of their vibrational spectra. The spectra have been measured *via* IR multiple photon dissociation of their complexes with Ar atoms in the 50–250 cm^{-1} range with an infrared free electron laser. Density functional theory calculations using a 4*f*-in-core effective core potential (ECP) accurately reproduce the experimental far-IR spectra. The ECP corresponds to a $4f^8 5d^1 6s^2$ trivalent configuration of terbium. The assigned structures are similar to those observed in several other transition metal systems. From this, we conclude that the bonding in Tb clusters is through the interactions between the 5*d* and 6*s* electrons, and that the 4*f* electrons have only an indirect effect on the cluster structures.

© 2013 American Institute of Physics. [<http://dx.doi.org/10.1063/1.4776768>]

Small clusters of lanthanide elements are promising materials for molecular magnets, due to their large magnetic moments and strong spin-orbit interaction.¹ The magnetism of lanthanide metal clusters originates from the Ruderman, Kittel, Kasuya, Yosida (RKKY) indirect exchange interaction,² and the magnetic anisotropy is primarily due to the interaction between the asymmetric 4*f* charge cloud and the local crystal field. Both of these properties are highly dependent on the geometric structure, and the lack of knowledge of the cluster structures is a major barrier to understanding their magnetism. To obtain fundamental insights into their properties, the clusters can be studied in gas-phase molecular beam experiments, which provide an environment free of external influences.

The magnetism of lanthanide clusters has been studied experimentally using the Stern-Gerlach deflection technique.³ These experiments demonstrated that lanthanide clusters⁴ have large size-dependent magnetic moments and in some cases, Curie temperatures much higher than the corresponding bulk materials. Theoretically, the Gd_{13} cluster has been most extensively studied: In Ref. 5, the cluster structures were taken to be fragments of the bulk hcp lattice, and the magnetism was described phenomenologically with a Heisenberg Hamiltonian. The exchange constants which describe the strength of the interaction between local 4*f* moments due to the RKKY interaction were taken as undetermined parameters, rather than properly estimated from electronic structure calculations. In fact, little to nothing is known about the physics of the RKKY interaction in small sub-nanometer particles. This situation stands in sharp contrast to the present understanding of the bulk lanthanides where many physical properties are well understood with simple models, and first-principles

theory can calculate magnetic ordering temperatures with near quantitative accuracy.^{2,6} The structures of the bulk lanthanides are all known from X-ray diffraction on single crystal and thin film samples, and the lack of such structural information is a major barrier preventing the application of high-level theory to small clusters. A recent theoretical study of the Gd_{13} cluster,⁷ which attempted to include the 4*f* electrons, concluded that the lowest energy structures were icosahedral, rather than hcp-like, contradicting the previous results of Ref. 5. Despite this, lanthanide clusters have received little or no attention from experimental structural studies.

State of the art computational electronic-structure theory still has many difficulties with reliable prediction of cluster structures and their related properties from first principles. This holds in particular for metals with partially filled *d* (transition metals) or *f* (lanthanides, actinides) shells or for heavy elements, such as gold, where relativistic effects are significant. Experimental data are therefore essential for testing the validity of predictions and in motivating methodological developments. To this end, hybrid experimental/theoretical studies with photoelectron spectroscopy,⁸ trapped-ion electron diffraction,⁹ and far-IR spectroscopy¹⁰⁻¹² have provided invaluable information on the structures of small metal clusters. To identify the cluster structures, we present here experimental far-IR vibrational spectra for cationic terbium clusters in the gas phase, mass-selectively measured by the dissociation of weakly bound Ar messenger complexes. This method has been successfully applied before, e.g., to transition metal clusters.^{10,11,13-16} Terbium was chosen because there is a single naturally occurring isotope, which is beneficial for mass spectrometric studies, and it can be reasonably expected to behave as a prototype for the heavy lanthanides^{2,17} (Gd, Tb, Dy, Ho, Er), which are all trivalent and have the same hcp bulk lattice type.

^{a)}Electronic mail: jbowlan@fhi-berlin.mpg.de.

The Free Electron Laser for Infrared eXperiments (FELIX) in Nieuwegein, the Netherlands, was used as the far-IR source for these experiments. The experimental setup and methods have been described in previous publications^{10,13} and we only give a brief summary of the relevant details here. Tb clusters are produced in a laser vaporization cluster source, which is in part cooled to 77 K. The He carrier gas is seeded with 5% Ar, which leads to the formation of a small population of weakly bound Ar complexes of the Tb_n^+ clusters. The cluster beam is irradiated by the tunable far-IR radiation from FELIX and mass analyzed with a reflectron time-of-flight mass spectrometer. The FELIX beam used in the experiment delivers an energy on the order of ≈ 10 mJ within a pulse of about 7–9 μ s duration. Mass spectra of alternating shots from the cluster source with FELIX toggled on and off are stored into separate channels of a digitizer and in total about 500 mass spectra are averaged per channel and frequency interval. The IR induced relative depletion of the mass signals for the Tb_n^+ -Ar complexes is evaluated as a function of IR frequency to obtain the size specific far-IR spectra.

The experimental IR spectra for Tb_n^+ ($n = 5-9$) are shown in Figs. 1–3. There are well-resolved absorption bands for most cluster sizes. The spectra of the smaller sizes, $n = 5, 6$, and 7, are dominated by a single intense feature, which may suggest a highly symmetric structure, while the larger sizes, $n = 8$ and 9 have more richly featured spectra. For the studied

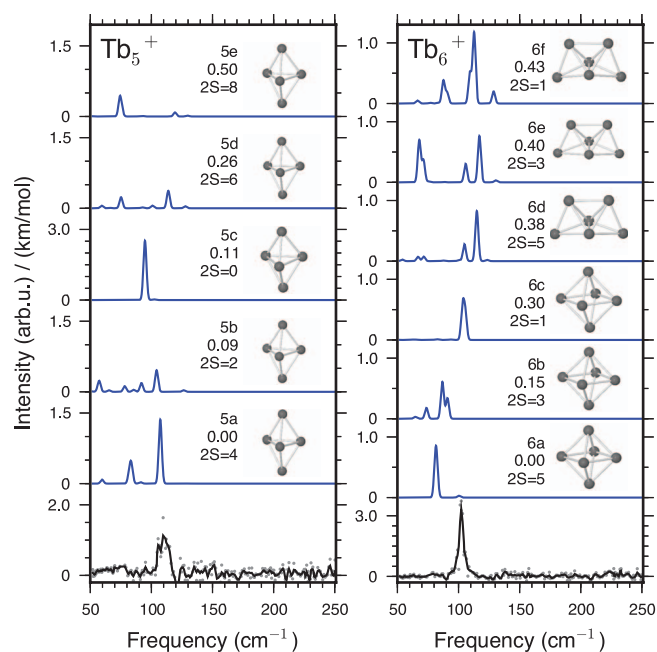


FIG. 1. Experimental far-IR spectra of Tb_5^+ and Tb_6^+ compared with the theoretically predicted spectra for a selection of low-lying structural isomers and $5d_6s$ spin states. The experimental spectra are shown in relative cross sections $\sigma \propto \nu/P(\nu) \log(I_0/I(\nu))$ derived from the depletion of the Ar complexes, normalized by the photon fluence. All experimental spectra are obtained from the complexes with a single Ar atom, except for Tb_5^+ where for intensity reasons the complex with two Ar atoms has been used. To help the eye, the experimental raw data points (gray dots) are overlaid with their 5 point running average. For each isomer, its energy relative to the lowest energy isomer identified (in eV) and the number of unpaired electrons $2S$ are given. The calculated stick spectrum is folded with a Gaussian line width function of 2 cm^{-1} full width at half maximum.

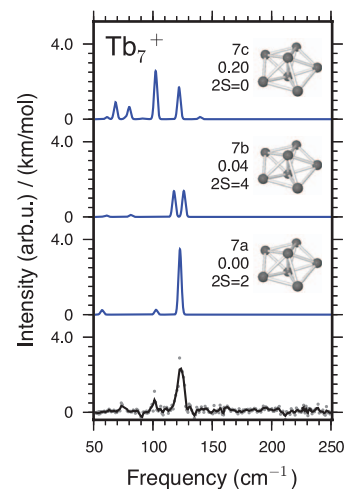


FIG. 2. Far-IR spectrum and comparison to predictions for different isomers of Tb_7^+ . Other plausible structures for Tb_7^+ , such as a capped octahedron, or bicapped pentagonal bipyramid are either significantly higher in energy, or converge to a pentagonal bipyramid under local optimization of the total energy.

cluster sizes, we find absorption bands in the 50–160 cm^{-1} range, which is approximately the range where the optical phonon branches of the bulk metal were observed by neutron scattering.¹⁸ With few exceptions, all observed metal cluster vibrations are below the reported value for the stretching frequency of the neutral Tb_2 of 137 cm^{-1} .¹⁹

To identify the clusters' structures based on the experimental spectra, we perform quantum chemical calculations using density functional theory (DFT). We use the Perdew-Burke-Ernzerhof (PBE) functional²⁰ for exchange and correlation as implemented in TURBOMOLE 6.2.²¹ The treatment of the $4f$ electrons with DFT remains a challenge because they

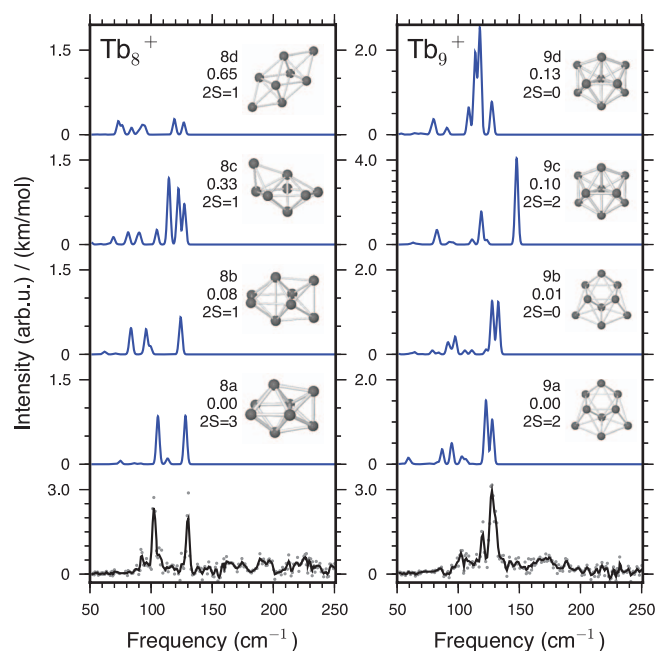


FIG. 3. Far-IR spectra and comparison to predictions for different isomers of Tb_8^+ and Tb_9^+ .

occupy an open shell and are highly localized to their parent atoms, where correlation effects are strong. Their strong localization also implies that they do not directly participate in chemical bonding. Standard DFT functionals are known to falsely delocalize the $4f$ electrons, and explicit treatment of the $4f$ states requires corrections such as LDA+U.²² Alternatively, it is possible to exploit the localization of the $4f$ states and treat them as a part of the core with an effective core potential. We follow this approach, using the *ECP54MWB* effective core potential developed by Dolg *et al.*²³ The valence orbitals are described with the $(6s6p5d)/[4s4p4d] + 2s1p1d$ (*ECP54MWB-II*) basis set.²⁴ The ECP includes 8 $4f$ electrons in the core. This corresponds to the commonly observed trivalent ($4f^8 5d^1 6s^2$) configuration of the terbium atom, which differs from the $4f^9 6s^2$ ground state of the neutral gas-phase Tb atom. The trivalent state is most commonly found for the heavy lanthanides in bulk and molecular form because the $4f \rightarrow 5d$ promotional energy is dominated by the bonding or cohesive energy of the $3 +$ state.¹⁷ We investigated the possibility of divalent Tb in our calculations using the *ECP55MWB* ECP, but found non-bonding or non-convergent structures.

For metal clusters, the interrogation of the configurational space becomes rapidly more complex with growing size and many locally stable arrangements of atoms, in addition to the true global minimum, may be identified for any given cluster size. We investigated a wide range of possible isomers starting our search with geometries that have been reported for transition metal clusters (after scaling the interatomic distances to values, which match the bulk values for Tb) including those that have been identified in our previous studies,^{10,11,13,14} followed by local optimization. In addition, for several sizes, we used Monte-Carlo basin-hopping sampling²⁵ to locate other local minima. No symmetry constraints have been applied. For all local minima found, the IR spectra have been calculated analytically based on the harmonic approximation; the frequencies are not further scaled. For $n = 5-7$, alternative isomers are typically much higher in energy. This suggests that the potential-energy surface is quite smooth.

An additional parameter of the calculations is the electronic occupation of the valence states. In all of these calculations, electronic states with different numbers of unpaired $5d/6s$ valence electrons have been considered in order to identify the preferred configuration. The spin states we refer to in the following only relate to the $5d/6s$ occupation as the $4f$ electrons are part of the ECP and not explicitly treated. If the $4f$ electrons were included, the total spin of any Tb cluster would be much higher. (The $4f$ shell of trivalent Tb has a configuration $J = 6$, $g_L = 3/2$ yielding a theoretical moment of $g_L \mu_B J = 9 \mu_B$ per atom.²) The ECP calculations also explicitly neglect any ordering of the $4f$ moments, as well as the $4f - (5d6s)$ exchange interaction, which is known to split the majority and minority ($5d6s$) spin states for bulk Tb metal in the ferromagnetic state by 0.1 eV.²² An exchange splitting of this magnitude could plausibly change the ground state valence occupation, and thus the far-IR spectra. The surprising fact is that the $4f$ -in-core model, which completely neglects this effect, still gives remarkably good agreement with the experimental spectrum. The frequencies of the IR active bands

are correctly predicted to within 1%, and the relative intensities match qualitatively. Figs. 1–3 show a comparison between the experimental far-IR spectra and those of the identified putative ground states. More isomers and their spectra calculated with a smaller *ECP54MWB*, presumably less accurate, basis set are reported in the supporting information.²⁶ In short, we can assign the following structures for Tb_{5-9}^+ (approximate symmetries are given in parentheses): 5–trigonal bipyramid (C_{2v} $2S = 4$), 6–distorted octahedron (**6c** – D_{2h} $2S = 1$), 7–pentagonal bipyramid or decahedron (D_{5h} $2S = 2$), 8–bicapped octahedron (D_{2d} $2S = 3$), 9–triccapped octahedron (C_{2v} $2S = 2$).

For the small clusters, Tb_{5-7}^+ , the best matches to the IR spectra are obtained with the putative ground states, which are calculated to have 4, 1, and 2 unpaired $5d/6s$ electrons, respectively. For a given structure, different spin states are often close in energy, but their calculated IR spectra can differ remarkably, as seen for Tb_8^+ . In this case, the doublet state **8b** is higher in energy than the quartet **8a**, but the spectrum of **8a** fits the experiment better. The presence of (several) unpaired $5d/6s$ electrons is consistent with Stern-Gerlach experiments³ on La and Y clusters,²⁷ which found many sizes with net magnetic moments ($0.2 \mu_B$ /atom). La and Y have very similar valence electronic structure to the lanthanides, but no $4f$ electrons. Thus, the observation of high spin in these clusters supports our finding, even without properly accounting for the possibility of a $5d6s$ spin polarization induced by the large localized $4f$ moments.

We find no evidence of multiple isomers for any of these small Tb clusters, although for Tb_9^+ there are several isomers based on two structural motifs (**9a/9b** and **9c/9d**), which are close in energy (within 0.2 eV) and which have similar spectra. The **9a/9b** is formed by capping three adjacent faces of an octahedron and **9c/9d** can be described as two interpenetrating decahedra. Both of these could be present, but structure **9a/9b** fits the experimental spectra better, and the energy difference of 0.1 eV is too small to be considered meaningful.

The lowest energy isomer identified by theory does not always give the best match to the theory, a case illustrated by Tb_6^+ . Tb_6^+ has 17 ($5d6s$) electrons, one fewer than the 18 needed to satisfy a spherical shell closing. This would indicate a preference for a low-spin distorted geometry **6c**, over the octahedral **6a**. However, the highly symmetric octahedral structure has high density of states at the HOMO, which increases the energy gained by exchange splitting in a high spin state. It is possible for this effect to stabilize a highly symmetric structure against a Jahn-Teller distortion. Indeed, the calculations predict that the $2S = 5$ octahedral structure **6a** is 0.3 eV lower in energy than the distorted low-spin ($2S = 1$) structure **6c**, but **6c** appears to match the experimental spectrum better. It is important to note, however, that the geometric difference between **6a** and **6c** is small, (the bond lengths differ by 2–5%) and their vibrational spectra are very similar. The octahedral structure **6a** actually has a triply degenerate vibrational mode located at 100 cm^{-1} , which is close to where an intense feature is observed in the experimental spectrum. However, the IR intensities calculated for these modes are very low. Further investigation is required to understand whether the presence of the Ar, or the inclusion of the $4f$

electrons would change the IR intensities of these modes. Thus, our experiment cannot determine conclusively whether Tb_6^+ is a perfect octahedron.

To conclude, we have demonstrated that far-IR spectroscopy allows for structural assignment for small lanthanide clusters. Our theoretical approach, where the $4f$ electrons are treated as a part of the core, predicts the frequencies and IR intensities of the cluster vibrational modes with remarkable accuracy. This confirms that, such as the bulk materials, the $4f$ electrons remain tightly localized in metal clusters and do not directly participate in bonding. The structures identified are similar to the geometries found for transition metal clusters. In this sense, heavy lanthanides behave like early transition metals with small d -occupation. It is also highly surprising that the structures can be determined while the magnetic order and $4f - (5d6s)$ exchange interaction are completely neglected. Knowledge of the cluster structures will enable the application of higher level theory for an explicit treatment of the $4f$ electrons, which in turn will provide a detailed understanding of lanthanide cluster magnetism.

We acknowledge the support of the Stichting voor Fundamenteel Onderzoek der Materie (FOM) for providing beam time on FELIX, and the FELIX staff for their skillful assistance, in particular B. Redlich and A. F. G. van der Meer. We acknowledge Marek Sierka, and Pekka Pyykkö for helpful discussions. J.B. and D.J.H. thank the Alexander von Humboldt foundation for financial support.

¹D. Gatteschi, *Nat. Chem.* **3**, 830 (2011); N. Ishikawa, M. Sugita, and W. Wernsdorfer, *Angew. Chem., Int. Ed.* **44**, 2931 (2005); P. H. Lin *et al.*, *ibid.* **120**, 8980 (2008); P. Lin *et al.*, *ibid.* **48**, 9489 (2009).

²J. Jensen and A. R. Mackintosh, *Rare Earth Magnetism* (Clarendon-Oxford, 1991).

³D. Douglass, J. Bucher, and L. Bloomfield, *Phys. Rev. Lett.* **68**, 1774 (1992); D. Gerion, A. Hirt, and A. Châtelain, *ibid.* **83**, 532 (1999); J. Bowlan *et al.*, *J. Appl. Phys.* **107**, 09B509 (2010); C. N. van Dijk *et al.*, *ibid.* **107**, 09B526 (2010).

⁴Gd, Tb, Dy, Pr, Ho, and Tm have been studied.

⁵D. Pappas *et al.*, *Phys. Rev. Lett.* **76**, 4332 (1996); V. Cerovski, S. Mahanti, and S. Khanna, *Eur. Phys. J. D* **10**, 119 (2000).

⁶I. D. Hughes *et al.*, *Nature (London)* **446**, 650 (2007).

⁷H. K. Yuan, H. Chen, A. L. Kuang, and B. Wu, *J. Chem. Phys.* **135**, 114512 (2011).

⁸J. Li, X. Li, H. J. Zhai, and L. S. Wang, *Science* **299**, 864 (2003); O. Kostko, B. Huber, M. Moseler, and B. von Issendorff, *Phys. Rev. Lett.* **98**, 43401 (2007).

⁹X. Xing, B. Yoon, U. Landman, and J. H. Parks, *Phys. Rev. B* **74**, 165423 (2006); M. P. Johansson, A. Lechtken, D. Schooss, M. M. Kappes, and F. Furch, *Phys. Rev. A* **77**, 053202 (2008).

¹⁰A. Fielicke *et al.*, *Phys. Rev. Lett.* **93**, 23401 (2004).

¹¹D. J. Harding *et al.*, *J. Chem. Phys.* **133**, 214304 (2010).

¹²P. Gruene *et al.*, *Science* **321**, 674 (2008).

¹³A. Fielicke *et al.*, *J. Chem. Phys.* **127**, 234306 (2007).

¹⁴D. J. Harding *et al.*, *J. Chem. Phys.* **132**, 011101 (2010).

¹⁵C. Ratsch *et al.*, *J. Chem. Phys.* **122**, 124302 (2005).

¹⁶P. Gruene, A. Fielicke, and G. Meijer, *J. Chem. Phys.* **127**, 234307 (2007).

¹⁷M. Domke *et al.*, *Phys. Rev. Lett.* **56**, 1287 (1986).

¹⁸J. C. G. Houmann and R. M. Nicklow, *Phys. Rev. B* **1**, 3943 (1970).

¹⁹J. R. Lombardi and B. Davis, *Chem. Rev.* **102**, 2431 (2002).

²⁰J. P. Perdew, K. Burke, and M. Ernzerhof, *Phys. Rev. Lett.* **77**, 3865 (1996).

²¹TURBOMOLE V6.2 2010, a development of University of Karlsruhe and Forschungszentrum Karlsruhe GmbH, 1989-2007, TURBOMOLE GmbH, since 2007; also available at <http://www.turbomole.com>.

²²K. M. Döbrich *et al.*, *Phys. Rev. B* **76**, 035123 (2007).

²³M. Dolg, H. Stoll, A. Savin, and H. Preuss, *Theor. Chim. Acta* **75**, 173 (1989); M. Dolg, H. Stoll, and H. Preuss, *ibid.* **85**, 441 (1993); J. Yang and M. Dolg, *ibid.* **113**, 212 (2005).

²⁴See <http://www.theochem.uni-stuttgart.de/pseudopotentials/> for the ECP and basis set.

²⁵D. J. Wales and J. P. K. Doye, *J. Phys. Chem. A* **101**, 5111 (1997).

²⁶See supplementary material at <http://dx.doi.org/10.1063/1.4776768> for atomic coordinates, energies, and calculated IR-spectra of all isomers.

²⁷M. B. Knickelbein, *Phys. Rev. B* **71**, 184442 (2005).